

# Covalent Immobilization and Characterization of Penicillin G Acylase on Magnetic NiFe<sub>2</sub>O<sub>4</sub> Nanorods Prepared via a Novel Rapid Combustion Process

R. J. Liu,<sup>a, b, \*</sup> Y. Li,<sup>a</sup> J. Han,<sup>a</sup> and H. X. Fu<sup>a</sup>

<sup>a</sup>School of Pharmacy, Jiangsu University, Zhenjiang 212013, P.R. China

<sup>b</sup>Affiliated Kunshan Hospital, Jiangsu University, Kunshan 215300, P.R. China

doi: 10.15255/CABEQ.2015.2319

Original scientific paper  
Received: November 1, 2015  
Accepted: December 5, 2016

The surface of magnetic NiFe<sub>2</sub>O<sub>4</sub> nanorods prepared via a novel rapid combustion process was modified by sodium silicate and glutaraldehyde, and the penicillin G acylase (PGA) was successfully immobilized on the surface-modified magnetic NiFe<sub>2</sub>O<sub>4</sub> nanorods. The properties of immobilized PGA were investigated, and the results showed that the immobilized PGA with high effective activity, good stability of enzyme catalyst, and good reusability was less affected by pH and temperature than free PGA. The immobilized PGA on magnetic NiFe<sub>2</sub>O<sub>4</sub> nanorods could be separated easily from the reaction solutions by the external magnetic field for cyclic utilization, and they could retain over 70 % of initial enzyme activity after 10 consecutive operations. All the results suggested that the surface-modified magnetic NiFe<sub>2</sub>O<sub>4</sub> nanorods would be promising for applications in the biomaterial fields.

*Key words:*

NiFe<sub>2</sub>O<sub>4</sub> nanorods, rapid combustion process, penicillin G acylase, immobilization

## Introduction

Penicillin G acylase (PGA, EC 3.5.1.11), an N-terminal nucleophile hydrolase with molecular dimensions of 7.0×5.0×5.5 nm<sup>3</sup>, is a significant catalyst in many pharmaceutical processes<sup>1,2</sup>, and it can remarkably catalyze the hydrolysis of amidic bonds of penicillin G to produce 6-aminopenicillanic acid (6-APA), which is an important intermediate for the production of β-lactam antibiotics<sup>3,4</sup>. However, the difficulties in separating it from the reaction mixture and cyclic utilization, product contamination because of enzyme, and thermal instability, etc., limit the application of the enzyme in industrial production. Therefore, as a solution enzyme, an efficient recovery and reuse of PGA is a prerequisite for its economic industrial applications. At this time, enzyme immobilization is raised in response to the proper time and conditions, which is considered one of the most biotechnological applications<sup>5</sup> and has attracted much attention.

Many organic or inorganic carriers have been used to immobilize PGA<sup>6</sup>, but the organic carriers have some inevitable disadvantages, such as poor stability towards organic solvents, microbial attacks, and disposal problems<sup>7</sup>. In contrast, many inorganic carriers, with high specific surface areas, large pore volume, and strong physical strength, are antimicrobial and stable towards organic solvents,

thus they are well fit for immobilization of enzyme. However, many nonmagnetic inorganic carriers should often be separated from the reaction mixture by special techniques; while nano- or micro- materials with magnetic properties have great potential applications because they can be separated rapidly and easily from reaction systems by applying an external magnetic field<sup>8</sup>.

At the same time, the ordinary immobilization methods, such as adsorption<sup>9</sup>, often lead to a lower utilization rate, while covalent crosslink may effectively enhance immobilization of enzyme<sup>10</sup>. The surface modification of magnetic nanomaterials is a key procedure, because it can make beneficial improvements in the surface properties, enzyme activity, and stability. Thus, in this work, the magnetic NiFe<sub>2</sub>O<sub>4</sub> nanorods were prepared via the rapid combustion process, the surface of the nanorods was modified, PGA was successfully immobilized on surface-modified magnetic NiFe<sub>2</sub>O<sub>4</sub> nanorods, and the properties of the immobilized PGA were investigated.

## Experimental

### Preparation and characterization of NiFe<sub>2</sub>O<sub>4</sub> nanorods

The magnetic NiFe<sub>2</sub>O<sub>4</sub> nanorods were prepared via the rapid combustion process. Typically, analytical-grade nickel nitrate and iron nitrate were used,

\*Corresponding author: Prof. Ruijiang Liu; E-mail address: luckystar\_lrj@ujs.edu.cn; Tel./fax: +86-511-85038201

and the molar ratio of Ni and Fe was 1:2. 2.48 g  $\text{Ni}(\text{NO}_3)_2 \cdot 6\text{H}_2\text{O}$ , and 6.89 g  $\text{Fe}(\text{NO}_3)_3 \cdot 9\text{H}_2\text{O}$  were dissolved in 10 mL of absolute alcohol, and the mixture was magnetically stirred for 2–4 h at room temperature to form a homogeneous solution. The solution was then put into a coppel and ignited. When the fire went out, the as-burnt intermediate with the coppel was calcined at 400 °C for 2 h at a heating rate of 3 °C  $\text{min}^{-1}$ .

The phase structure and phase purity of the as-prepared nanorods were examined by X-ray diffraction (XRD) (Holland Philips X'pert X-ray diffractometer with Cu K $\alpha$  radiation,  $\lambda = 1.5406 \text{ \AA}$ ) at 40 kV, 30 mA over the  $2\theta$  range 20–80°. Morphology and composition analysis were conducted with transmission electron microscopy (TEM). Magnetic measurement of the samples in the powder form was carried out at room temperature using a vibrating sample magnetometry with a maximum magnetic field of 10 kOe.

#### Surface modification of magnetic $\text{NiFe}_2\text{O}_4$ nanorods

For immobilization of PGA, the silica-coated  $\text{NiFe}_2\text{O}_4$  nanorods were prepared. An amount of 1.0 g of  $\text{NiFe}_2\text{O}_4$  nanorods were suspended in 200 mL double distilled water, and then heated to 80 °C. An amount of 20 mL of 1.0 mol  $\text{L}^{-1}$  sodium silicate was added dropwise into the solution, which was adjusted to pH 6.0 with 2 mol  $\text{L}^{-1}$  HCl solution within 2 h. After another 3 h of stirring, the obtained silica-coated  $\text{NiFe}_2\text{O}_4$  nanorods were washed with double distilled water and collected by magnetic separation, followed by drying at 50 °C under vacuum for 12 h. Finally, the  $\text{NiFe}_2\text{O}_4@ \text{SiO}_2$  nanocomposites were obtained.

To obtain the aldehyde-functionalized  $\text{NiFe}_2\text{O}_4@ \text{SiO}_2$  nanocomposites, glutaraldehyde was

used as the reagent for surface modification of  $\text{NiFe}_2\text{O}_4@ \text{SiO}_2$  nanocomposites. Typically, 0.1 g  $\text{NiFe}_2\text{O}_4@ \text{SiO}_2$  nanocomposites were suspended in 1 mL of 50 mmol  $\text{L}^{-1}$  phosphate buffer with pH 7.0, and then 0.2 mL glutaraldehyde of 25 % was added and mixed well for 2 h at room temperature. After being thoroughly washed with 1 mol  $\text{L}^{-1}$  sodium chloride solution prepared with 50 mmol  $\text{L}^{-1}$  phosphate buffer with pH 7.0, the resulting materials were feasible for immobilization of PGA.

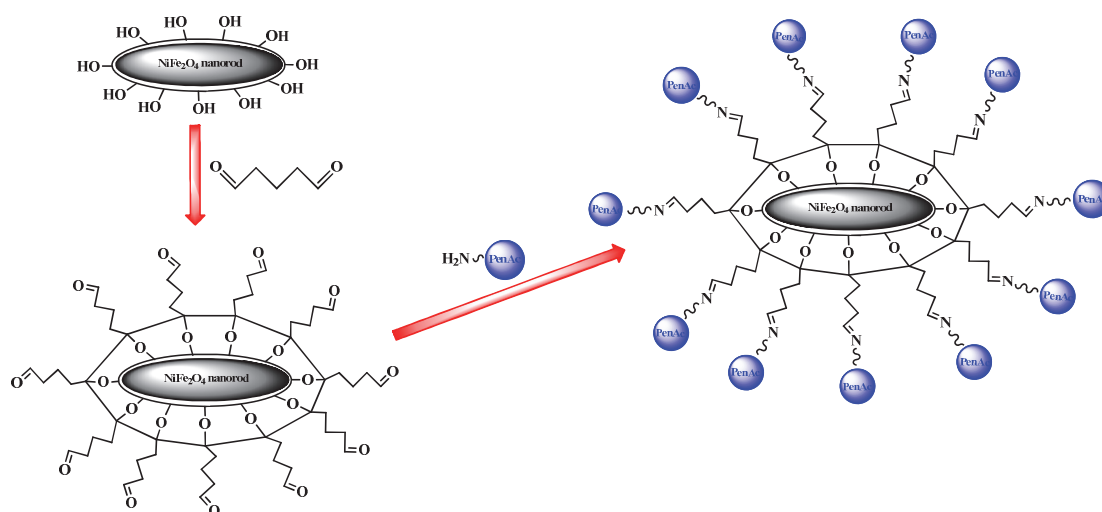
The procedure for immobilization of PGA onto core-shell magnetic  $\text{NiFe}_2\text{O}_4@ \text{SiO}_2$  nanocomposites is shown in Scheme 1.

#### Protein concentration assay

Protein concentration was measured with the Biorad Protein assay using bovine serum albumin as standard<sup>11</sup>. An amount of 0.1 mL PGA solution was diluted 150 times with double distilled water, and then the diluted PGA solutions of 0.1, 0.2, 0.3, 0.4, 0.5, 0.6, 0.7, 0.8 mL were put into eight test tubes. An 0.9 % sodium chloride solution was added to reach 1.0 mL for each tube, and 5 mL Coomassie brilliant blue solution was added into the above solutions, respectively. Compared with blank solution of 0.9 % sodium chloride, the absorbances were determined by the wavelength of 595 nm. The experiments were repeated three times, and according to the relationship between the average absorbance and the concentration of protein, the concentration of free enzyme was calculated.

#### Enzyme assay

The activity of PGA was determined by the colorimetric method proposed by Balasingham *et al.*<sup>12</sup>, and one unit (U) of PGA is defined as the amount of enzyme that can produce 1 mmol 6-APA



Scheme 1 – Immobilization procedure of PGA onto magnetic  $\text{NiFe}_2\text{O}_4@ \text{SiO}_2$  nanocomposites

per min with 4 % (w/v) penicillin G as substrate solvated in phosphate buffer with pH 8.0 at 37 °C<sup>13,14</sup>. The amount of 6-APA was determined with the method of p-dimethylaminobenzaldehyde (PDAB)<sup>15</sup>. The solution mixture of 100 mL methanol, 50 mL of 2 mol L<sup>-1</sup> NaOH, and 0.5 g PDAB was diluted to 700 mL, and the PDAB solution was prepared. The PGA solution was put into a narrow-neck flask at 37 °C, and 2 mL phosphate buffer with pH 8.0 and 5 mL of 4 % PGA solution were added. After 5 min, 1 mL of the reaction solution was taken out and diluted 105 times. Then, 0.5 mL of the diluted solution was taken out, and mixed with 3.5 mL PDAB solution for 5 min. Compared with blank solution, the absorbances were determined by the wavelength of 415 nm. According to the relationship between absorbance and the concentration of 6-APA, the activity of free PGA could be calculated. The experiments of enzyme assay were performed in triplicate.

### Immobilization of PGA

An amount of 0.1 g aldehyde-functionalized NiFe<sub>2</sub>O<sub>4</sub>@SiO<sub>2</sub> nanorods was suspended in 0.8 mL enzyme solution and well mixed at various temperatures. The immobilized PGA was separated by applying an external magnetic field, and washed 5 times using the 50 mmol L<sup>-1</sup> phosphate buffer with pH 7.0, which had 24 h incubation. The protein concentration and volume of the supernatant were measured to calculate the immobilization yield, as shown in the following equation (1)<sup>16</sup>.

$$\text{Immobilization yield} = \frac{A_1 - A_2}{A_1} \cdot 100 \% \quad (1)$$

where  $A_1$  is the total protein content of enzyme added in the initial immobilization solution,  $A_2$  is the protein content of the residual enzyme in the immobilization and washed solutions after the immobilization procedure.

### Activity of immobilized PGA

The measurement of immobilized PGA activity was similar to that mentioned in the section of enzyme assay. The maximum activities of free PGA and immobilized PGA were defined as 100 %, and the relative activities referred to the percentages of the activities of immobilized PGA accounting for the maximum one. The determination experiments of enzyme activity were repeated three times.

### Thermal stability of free PGA and immobilized PGA

An amount of 2 mL phosphate buffer with pH 8.0 was added into 4 μL free PGA or 0.1 g immobilized PGA, and enzyme preparations were incubated at various temperatures. The samples were with-

drawn periodically, and enzyme activity was analyzed as mentioned previously. PGA residual activity was expressed as a percentage of initial activity at the given incubation time. All experiments for thermal stability at various temperatures were investigated three times.

### Kinetic parameters determination of free PGA and immobilized PGA

Kinetic study was performed on selected samples in the substrate concentration range of 0.05 to 1.0 % (w/v) with 0.4 μL free PGA and 0.1 g immobilized PGA. The Michaelis-Menten equation for a single substrate, uninhibited enzyme reaction was used, as shown in equation (2).

$$v = \frac{v_{\max} [S]}{K_m + [S]} \quad (2)$$

where  $v$  is the rate of the reaction,  $[S]$  is the concentration of the substrate,  $K_m$  is the apparent constant, and  $v_{\max}$  is the maximum of reaction velocity. The Lineweaver-Burk plot for the Michaelis-Menten equation can be expressed as equation (3).

$$\frac{1}{v} = \frac{K_m}{v_{\max}} \cdot \frac{1}{[S]} + \frac{1}{v_{\max}} \quad (3)$$

### Recovery performance of immobilized PGA

The recovery performance of immobilized PGA was examined by conducting the activity measurement of immobilized PGA at 37 °C at intervals of 5 min. Also, activity measurements were carried out subsequently after each activity measurement. The immobilized PGA was separated magnetically, and then 2 mL phosphate buffer (pH 8.0) and 5 mL potassium salt (4 wt %) were added to the immobilized PGA.

## Results and discussion

### Characteristics of magnetic NiFe<sub>2</sub>O<sub>4</sub> nanorods and immobilized PGA

The characteristics for magnetic NiFe<sub>2</sub>O<sub>4</sub> nanorods are shown in Fig. 1. The TEM image of the magnetic NiFe<sub>2</sub>O<sub>4</sub> nanorods are shown in Fig. 1(a), and it could be seen that the average length of the magnetic NiFe<sub>2</sub>O<sub>4</sub> nanorods was about 130 nm, their diameter was about 25 nm. The selected area electron diffraction (SAED) pattern shown in Fig. 1(b) indicated that the prepared NiFe<sub>2</sub>O<sub>4</sub> nanorods had a single-phase spinel structure. The XRD pattern displayed in Fig. 1(c) showed that all the diffraction peaks could be indexed to spinel NiFe<sub>2</sub>O<sub>4</sub> (JCPDS No. 86-2267). According to the strongest

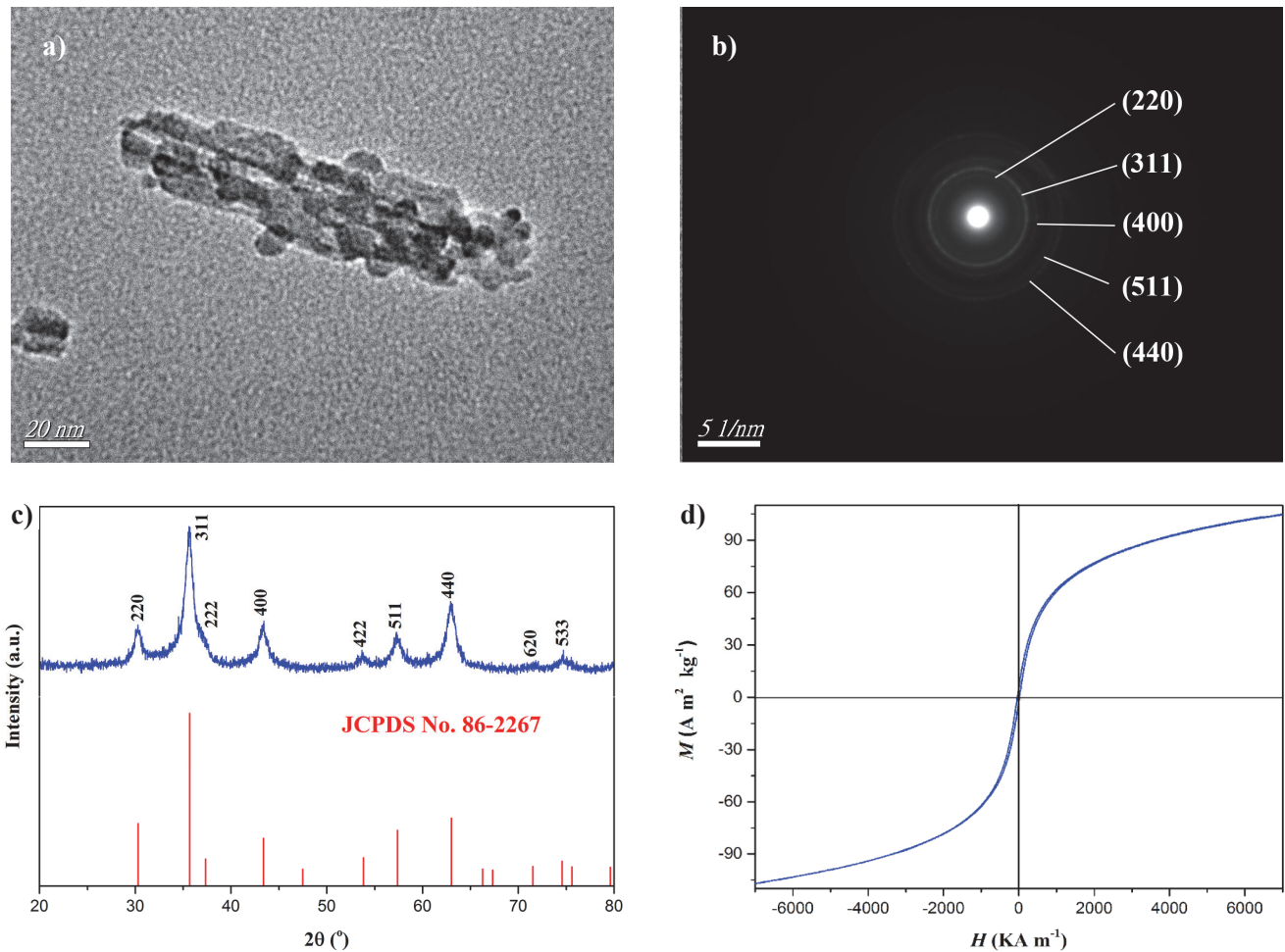


Fig. 1 – Characteristics of magnetic  $\text{NiFe}_2\text{O}_4$  nanorods: (a) TEM micrograph, (b) SAED pattern, (c) XRD pattern, and (d) Hysteresis loop

diffraction peak (311) data, the average crystalline size could be estimated by the Scherrer formula ( $D = K\lambda / B \cos\theta$ , where  $K$  is the Scherrer constant of 0.89,  $\lambda$  is the wavelength of the X-ray radiation,  $B$  is the full width at half maximum (FWHM) of the relevant reflection peak, and  $\theta$  is the diffraction angle.). The calculated average crystalline size for the  $\text{NiFe}_2\text{O}_4$  nanorods was 15 nm. Fig. 1(d) shows the hysteresis loops of the  $\text{NiFe}_2\text{O}_4$  nanorods with a typical soft magnetization behavior and the high magnetization ( $M_s$ ) of  $105.2 \text{ A m}^2 \text{ kg}^{-1}$ , which was almost twice that of magnetic  $\text{NiFe}_2\text{O}_4$  nanoparticles<sup>17</sup>, and after modification with silica, the high magnetization ( $M_s$ ) of magnetic  $\text{NiFe}_2\text{O}_4/\text{SiO}_2$  nanocomposites decreased to  $89.3 \text{ A m}^2 \text{ kg}^{-1}$ .

#### Optimization of immobilization time, and concentration of PGA

The technology of immobilization was optimized at various times of 3–24 h, and concentration range of PGA from  $1.0$  to  $3.5 \text{ mg mL}^{-1}$  at  $37^\circ\text{C}$ . Fig. 2 shows the effects of immobilization time (a) and PGA concentration (b) on activity of immobi-

lized PGA and immobilization yield. Fig. 2(a) shows that the activity of immobilized PGA and the immobilization yield at 6 h were highest and largest, while Fig. 2(b) shows that the activity of immobilized PGA was the highest when the PGA concentration was  $1.0 \text{ mg mL}^{-1}$ , however, the immobilization yield began to decrease. According to comprehensive consideration of these two findings, the immobilized PGA displayed the highest activity with immobilization time of 6 h and immobilization concentration of  $1.0 \text{ mg mL}^{-1}$ .

#### Effect of pH and temperature on activity of free PGA and immobilized PGA

The relative activities of the immobilized PGA were determined in the solutions at different pH ranging from 6 to 9.5, and various temperatures ranging from  $20$  to  $60^\circ\text{C}$ . Fig. 3 shows the effect of pH and temperature on the relative activities of free PGA and immobilized PGA. The optimum pH value and immobilization temperature were pH 8.0 and  $45^\circ\text{C}$ , respectively. From Fig. 3, it could be seen that the activity of immobilized PGA was less af-

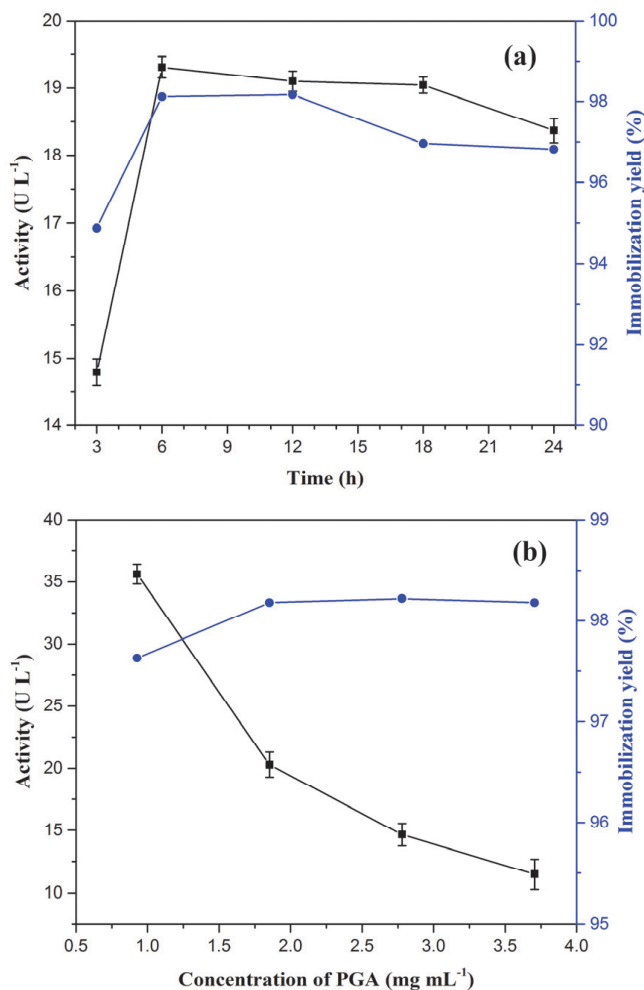


Fig. 2 – Effects of immobilization time (a) and PGA concentration (b) on activity of immobilized PGA (■) and immobilization yield (●)

ected by pH and temperature than that of free PGA, which revealed that immobilization of PGA magnetic NiFe<sub>2</sub>O<sub>4</sub> nanorods had significance.

#### Thermal stability of free PGA and immobilized PGA

Thermal stability of free PGA and immobilized PGA was measured with pH 8.0 at various temperatures. Fig. 4 showed the thermal stability of free PGA and immobilized PGA incubated in 0.1 mol L<sup>-1</sup> phosphate buffer (pH 8.0) at various temperatures and times. From Fig. 4, it could be seen that the activity of free PGA and immobilized PGA descended with the increase in temperature, and the activity was slightly affected at 30 °C and 40 °C, while it was more affected at higher temperatures. At the same time, the free PGA would lose the activity at 60 °C in 2 hours, however, the immobilized PGA could maintain over 50 % relative activity and had activity even after 8 hours, which revealed that immobilization of PGA onto magnetic NiFe<sub>2</sub>O<sub>4</sub> nanorods could enhance the activity of heat-resistance.

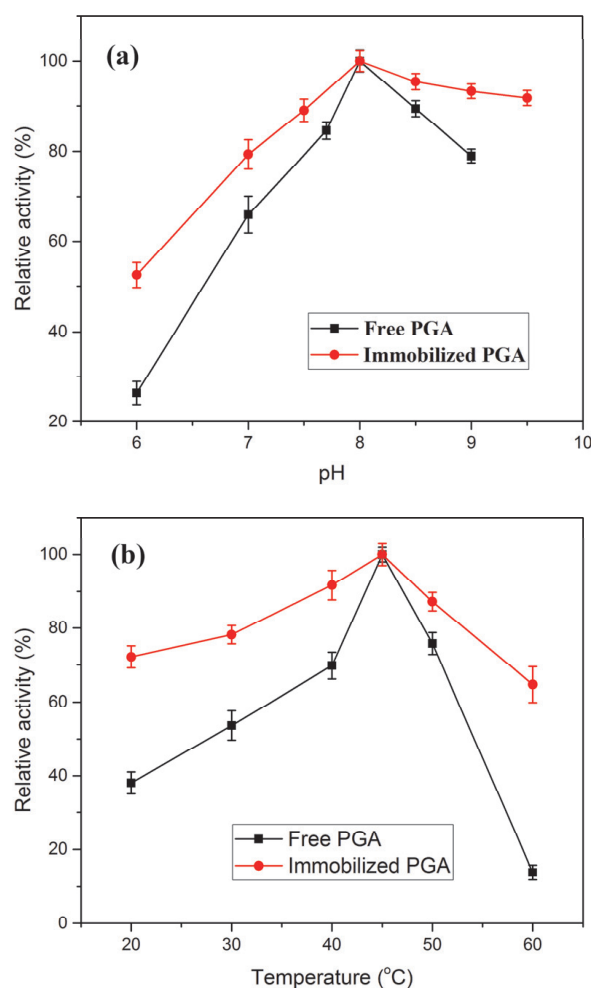


Fig. 3 – Effects of (a) pH and (b) temperature on activities of free PGA and immobilized PGA

#### Kinetic parameters of free PGA and immobilized PGA

The kinetic parameters ( $K_m$  and  $v_{max}$ ) of enzyme undergo variations after immobilization in general, which indicates a change in affinity for the substrate. These variations might occur due to several factors, such as protein conformational changes induced by the attachment to the support, steric hindrances, and diffusional effects. These factors lead to decrease or increase in the value of apparent  $K_m$ . The decrease in  $K_m$  indicated a faster reaction rate, whereas the increase in  $K_m$  suggested the requirement of higher substrate concentration to achieve the same reaction rate observed for the free enzyme<sup>18</sup>.

The kinetic parameters  $K_m$  and  $v_{max}$  values were determined from the Lineweaver-Burk plots, Hanes-Woolf plots for free PGA and immobilized PGA, shown in Fig. 5. The  $v_{max}$  value of the immobilized PGA (2.783 mmol mg<sup>-1</sup> min<sup>-1</sup>) was about 3.3 times higher than that of the free PGA (0.837 mmol mg<sup>-1</sup>

min<sup>-1</sup>); The  $K_m$  for the immobilized PGA (275.5 mmol L<sup>-1</sup>) was around 19.4 times higher than that of the free PGA (14.2 mmol L<sup>-1</sup>). The great increase in  $K_m$  indicating a lower substrate affinity of the immobilized PGA revealed that it was necessary to use higher substrate concentration to achieve the same velocity.

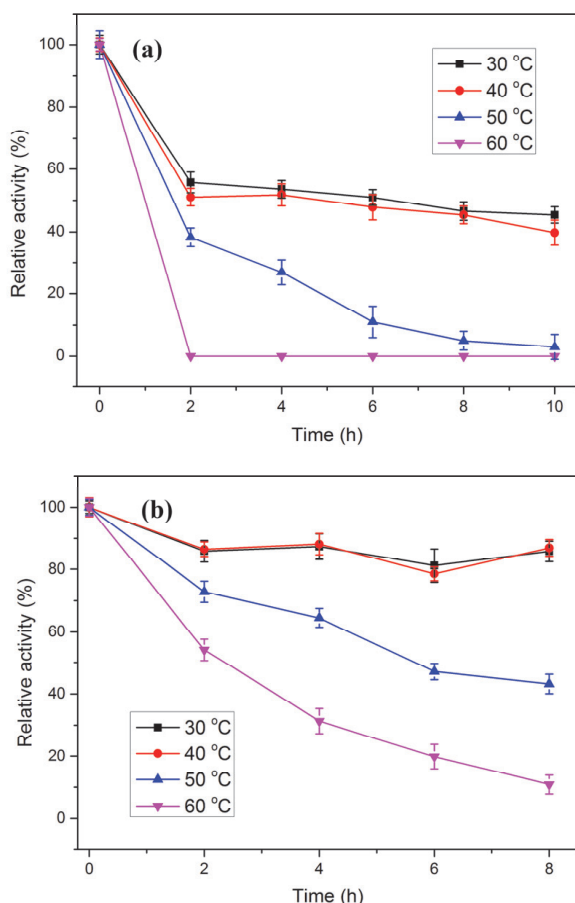


Fig. 4 – Thermal stabilities of (a) free PGA and (b) immobilized PGA incubated in 0.1 mol L<sup>-1</sup> phosphate buffer (pH 8.0) at various temperatures and times

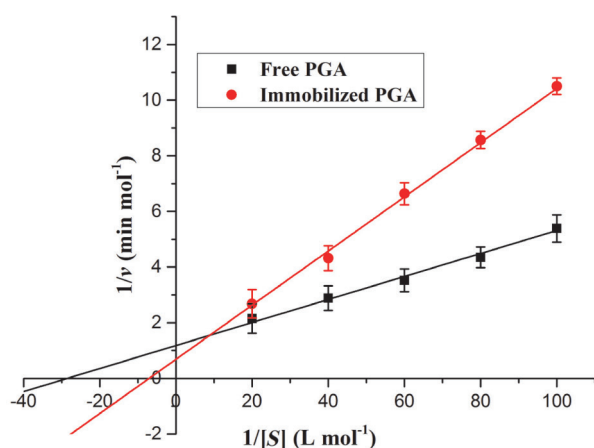


Fig. 5 – Hanes-Woolf plots for free PGA and immobilized PGA

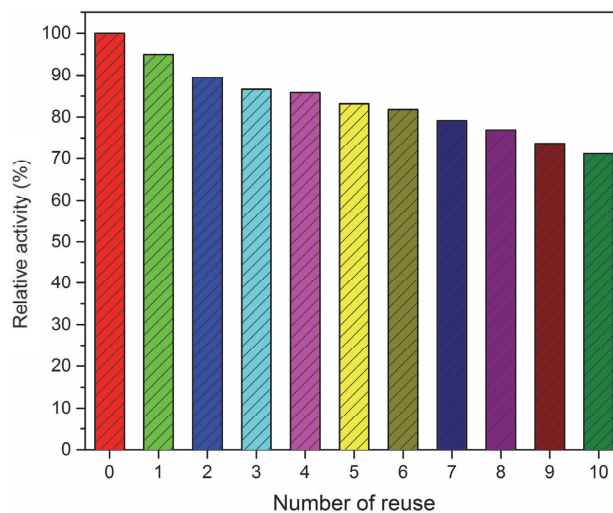


Fig. 6 – Reusability of immobilized PGA

### Reusability of immobilized PGA

The most significant and attractive advantage of immobilizing enzyme is the recycling property. The catalyst reusability was determined by measuring the activity of the immobilized PGA as a function of the number of reuses, since the immobilized PGA was separated by external magnetic field and reused in the next experiment. The residual activity of the immobilized PGA during the reuse is shown in Fig. 6. The immobilized PGA retained over 70 % residual activity after being used 10 times, which was larger than that of penicillin G acylase on magnetic Fe<sub>3</sub>O<sub>4</sub> nanoparticles modified by ionic liquids<sup>19</sup>, and basically reached the level of penicillin G acylase on aldehyde-functionalized mesoporous silica-Fe<sub>3</sub>O<sub>4</sub> nanocomposites<sup>20</sup>. The high recycle relative activity revealed that the reusability of the immobilized PGA was better than that of free PGA.

### Conclusions

(1) Magnetic NiFe<sub>2</sub>O<sub>4</sub> nanorods with average length of about 130 nm and diameter of about 25 nm were successfully prepared via the novel rapid combustion process, their surface was modified by sodium silicate and glutaraldehyde, and PGA was immobilized successfully onto the nanorods.

(2) The immobilized PGA exhibited high effective activity, good stability of enzyme catalyst, easy separation from the reaction mixture, and good reusability. The immobilization of PGA on surface-modified magnetic NiFe<sub>2</sub>O<sub>4</sub> nanorods prepared via the solution combustion process gives a new support providing excellent immobilization of the enzyme catalysts, which provides a novel, simple, and green process for the preparation of magnetic nanomaterials and immobilization of the enzyme, and will be promising for applications in the biomaterial fields.

## ACKNOWLEDGEMENTS

This work was supported by the China Postdoctoral Science Foundation (Grant No. 2016M591778), Jiangsu Postdoctoral Foundation (Grant No. 1501086C), and the Technology Development Project of Jiangsu ZTE Pharmaceutical Co., Ltd.

## References

1. Gao, Z. Y., Zhan, W. C., Wang, Y. S., Guo, Y., Wang, L., Guo, Y. L., Lu, G. Z., Aldehyde-functionalized mesostructured cellular foams prepared by copolymerization method for immobilization of penicillin G acylase, *Micropor. Mesopor. Mat.* **202** (2015) 90.  
doi: <https://doi.org/10.1016/j.micromeso.2014.09.053>
2. Yang, L., Gao, Z. Y., Guo, Y. L., Zhan, W. C., Guo, Y., Wang, Y. S., Lu, G. Z., Immobilization of penicillin G acylase on paramagnetic aldehyde-functionalized mesostructured cellular foams, *Enzyme Microb. Tech.* **60** (2014) 32.  
doi: <https://doi.org/10.1016/j.enzmictec.2014.03.011>
3. Yang, L., Gao, Z. Y., Guo, Y. L., Zhan, W. C., Guo, Y., Wang, Y. S., Lu, G. Z., Paramagnetic epoxy-functionalized mesostructured cellular foams with an open pore system for immobilization of penicillin G acylase, *Micropor. Mesopor. Mat.* **190** (2014) 17.  
doi: <https://doi.org/10.1016/j.micromeso.2014.01.017>
4. Magdy, M. M. E., Marwa, I. W., Magdy, A. A., Ahmed, I. E., Application of Plackett-Burman screening design to the modeling of grafted alginate-carrageenan beads for the immobilization of penicillin G acylase, *J. Appl. Polym. Sci.* **131** (2014) 40295.
5. Mohy Eldin, M. S., El Enshasy, H. A., Hassan, M. E., Haroun, B., Hassan, E. A., Covalent immobilization of penicillin G acylase onto amine-functionalized PVC membranes for 6-APA production from penicillin hydrolysis process. II. Enzyme immobilization and characterization, *J. Appl. Polym. Sci.* **125** (2012) 3820.  
doi: <https://doi.org/10.1002/app.36690>
6. Chong, A. S. M., Zhao, X. S., Design of large-pore mesoporous materials for immobilization of penicillin G acylase biocatalyst, *Catal. Today* **93** (2004) 293.  
doi: <https://doi.org/10.1016/j.cattod.2004.06.064>
7. Wang, W., Deng, L., Peng, Z. H., Xiao, X., Study of the epoxydized magnetic hydroxyl particles as a carrier for immobilizing penicillin G acylase, *Enzyme Microb. Tech.* **40** (2007) 255.  
doi: <https://doi.org/10.1016/j.enzmictec.2006.04.020>
8. Zhou, H. C., Li, W., Shou, Q. H., Gao, H. S., Xu, P., Deng, F. L., Liu, H. Z., Immobilization of penicillin G acylase on magnetic nanoparticles modified by ionic liquids, *Chinese J. Chem. Eng.* **20** (2012) 146.  
doi: [https://doi.org/10.1016/S1004-9541\(12\)60374-7](https://doi.org/10.1016/S1004-9541(12)60374-7)
9. Wang, P. X., Gong, X. Y., Su, E. Z., Xie, J. L., Wei, D. Z., A facile pretreatment method for efficient immobilization of penicillin G acylase, *Biochem. Eng. J.* **56** (2011) 17.  
doi: <https://doi.org/10.1016/j.bej.2011.04.011>
10. Zhao, J. Q., Wang, Y. J., Luo, G. S., Zhu, S. L., Covalent immobilization of penicillin G acylase on aminopropyl-functionalized mesostructured cellular foams, *Bioresource Technol.* **101** (2010) 7211.  
doi: <https://doi.org/10.1016/j.biortech.2010.04.067>
11. Bradford, M. M., A rapid and sensitive method for the quantitation of micro-gram quantities of protein utilizing the principle of protein-dye binding, *Anal. Biochem.* **72** (1976) 248.  
doi: [https://doi.org/10.1016/0003-2697\(76\)90527-3](https://doi.org/10.1016/0003-2697(76)90527-3)
12. Balasingham, K., Warburton, D., Dunnill, P., Lilly, M. D., The isolation and kinetics of penicillin amidase from *Escherichia coli*, *Biochim. Biophys. Acta.* **276** (1972) 250.  
doi: [https://doi.org/10.1016/0005-2744\(72\)90027-7](https://doi.org/10.1016/0005-2744(72)90027-7)
13. Zhan, W. C., Lü, Y. J., Yang, L., Guo, Y. L., Wang, Y. Q., Guo, Y., Lu, G. Z., Epoxidation of vinyl functionalized cubic Ia3d mesoporous silica for immobilization of penicillin G acylase, *Chinese J. Catal.* **35** (2014) 1709.  
doi: [https://doi.org/10.1016/S1872-2067\(14\)60156-X](https://doi.org/10.1016/S1872-2067(14)60156-X)
14. Luo, X. G., Zhang, L. N., Immobilization of penicillin G acylase in epoxy-activated magnetic cellulose microspheres for improvement of biocatalytic stability and activities, *Biomacromolecules* **11** (2010) 2896.  
doi: <https://doi.org/10.1021/bm100642y>
15. Wang, H., Jiang, Y. J., Zhou, L. Y., He, Y., Gao, J., Immobilization of penicillin G acylase on macrocellular heterogeneous silica-based monoliths, *J. Mol. Catal. B. Enzym.* **96** (2013) 1.  
doi: <https://doi.org/10.1016/j.molcatb.2013.06.005>
16. Shi, B. F., Wang, Y. S., Guo, Y. L., Wang, Y. Q., Wang, Y., Guo, Y., Zhang, Z. G., Liu, X. H., Lu, G. Z., Aminopropyl-functionalized silicas synthesized by W/O microemulsion for immobilization of penicillin G acylase, *Catal. Today* **148** (2009) 184.  
doi: <https://doi.org/10.1016/j.cattod.2009.02.014>
17. Sivakumar, P., Ramesh, R., Ramanand, A., Ponnusamy, S., Muthamizchelvan, C., Preparation and properties of nickel ferrite (NiFe<sub>2</sub>O<sub>4</sub>) nanoparticles via sol-gel auto-combustion method, *Mater. Res. Bull.* **46** (2011) 2204.  
doi: <https://doi.org/10.1016/j.materresbull.2011.09.010>
18. Adikane, H. V., Thakar, D. M., Studies of penicillin G acylase immobilization using highly porous cellulose-based polymeric membrane, *Appl. Biochem. Biotech.* **160** (2010) 1130.  
doi: <https://doi.org/10.1007/s12010-009-8686-9>
19. Zhou, H. C., Li, W., Shou, Q. H., Gao, H. S., Xu, P., Deng, F. L., Liu, H. Z., Immobilization of penicillin G acylase on magnetic nanoparticles modified by ionic liquids, *Chinese J. Chem. Eng.* **20** (2012) 146.  
doi: [https://doi.org/10.1016/S1004-9541\(12\)60374-7](https://doi.org/10.1016/S1004-9541(12)60374-7)
20. Yang, L., Guo, Y. L., Zhan, W. C., Guo, Y., Wang, Y. S., Lu, G. Z., One-pot synthesis of aldehyde-functionalized mesoporous silica-Fe<sub>3</sub>O<sub>4</sub> nanocomposites for immobilization of penicillin G acylase, *Micropor. Mesopor. Mat.* **197** (2014) 1.  
doi: <https://doi.org/10.1016/j.micromeso.2014.05.044>